Monosialoganglioside-GM1 triggers binding of the amyloid-protein salmon calcitonin to a Langmuir membrane model mimicking the occurrence of lipid-rafts

Marco Diociaiuti[a,*], Cristiano Giordani[a,b], Gihan S. Kamel[c,d], Francesco Brasili[d], Simona Sennato[d], Cecilia Bombelli[e], Karen Y. Meneses[b], Marco A. Giraldo[b], Federico Bordi[d]

[a] Dipartimento di Tecnologie e Salute, Istituto Superiore di Sanità, I-00161 Roma, Italy
[b] Instituto de Física, Universidad de Antioquia, Medellín, Colombia
[c] Department of Physics, Faculty of Science, Helwan University, Cairo, Egypt
[d] Dipartimento di Fisica and ISC-CNR, Sapienza Università di Roma, I-00185 Roma, Italy
[e] CNR, Istituto di Metodologie Chìmiche, Sezione Meccanismi di Reazione, c/o Dipartimento di Chimica, Università degli Studi di Roma "Sapienza", I-00185 Roma, Italy

ARTICLE INFO

ABSTRACT

GM1 ganglioside is known to be involved in the amyloid-associated diseases and it is a crucial factor for the assembly of amyloid proteins on lipid-rafts, which are lipid structures located on the synaptic plasma membranes. Due to its slow aggregation rate, we employed salmon calcitonin (sCT) as a suitable probe representative of amyloid proteins, to study the interaction between this class of proteins and a membrane model. Here, we prepared a neuronal membrane model by depositing onto mica two Langmuir-Blodgett films in liquid-condensed phase: the outer monolayer was characterized by high content of GM1 (50%) and minority parts of cholesterol and POPC (25–25%), while the inner one by plain POPC. To deeply investigate the interaction of sCT with this model and the role-played by GM1, we prepared the outer leaflet adding sCT at a concentration such that the number of proteins equals that of GM1. Atomic Force Microscopy revealed the occurrence of two distinct kinds of flat surfaces, with globular aggregates localized exclusively on top of the highest one. To unravel the nature of the interaction, we studied by ζ-potential technique liposomes composed as the outer leaflet of the model. Results demonstrated that an electrostatic interaction sCT-GM1 occurred. Finally, to investigate the interaction thermodynamics between sCT and the outer leaflet, Langmuir films as the outer monolayer and containing increasing content of sCT were studied by compression isotherms and Brewster Angle Microscopy experiments. Based on the all body of results we propose an interaction model where GM1 plays a pivotal role.

1. Introduction

It has been recently pointed out that "almost every human protein has segments that can form amyloid" and apparently a universal mechanism is responsible for β-sheet formation in globular proteins and fibrillar aggregates. In fact, practically all-complex proteins have six-aminoacid-long segments with the particular structure that prompts aggregation when the protein partly unfolds [1,2]. Goldschmidt and co-workers speculated that most proteins have evolved so that their structure effectively conceals their amyloid-prone areas, and that this mechanism was apparently ineffective for about 50 amyloid-disease associated proteins [2].

Misfolded proteins have the ability to aggregate and interact with plasma membranes, inducing cell damage and malfunction mainly mediated via the formation of ion channels. Interestingly, this kind of toxicity named "hydrophobicity-based" is similar to those described for bacterial pore-forming toxins and viral proteins [3–5].

Noticeably, Bucciantini et al. proved that proteins not associated with any disease are also neurotoxic, suggesting that a shared structural feature leading to the exposure of hydrophobic regions is at the basis of neurotoxicity, independently of their primary sequences [6,7].

Many studies have been carried out to investigate the relationship between structural features and toxicity of amyloid proteins involved in

amyloid-associated diseases (e.g. Alzheimer's disease) [8]. In the case of neurodegenerative-diseases, it is now generally accepted that the pathogenic aggregates are not the mature fibrils, but the intermediate soluble oligomers [9–11].

However, not only the protein structure seems to be involved in the molecular mechanisms of neurotoxicity and peculiar structures of the neuronal membrane are now under investigation. More in particular, the so-called "lipid-rafts" has apparently an important role in the pathogenicity.

It is well known that domains that generally not exceed 200 nm, enriched with sphingolipids, cholesterol (Chol) and characterized by high concentrations of membrane proteins, could exist. Lipid-rafts are not considered stable structures and the debate concerning their formation, dynamic, timeframe and composition is still open [12–17].

For what concerns the lipid component, it is now currently accepted that lipid-rafts represent a liquid-ordered (L_o) phase, made of un-saturated molecules like GM1 reinforced by Chol inserted in the hydrophobic backbone, floating in a more fluid liquid-expanded (L_e) phase made of unsaturated lipids [16–18].

As far as neurodegenerative diseases are concerned, lipid-rafts have been implicated in amyloidogenesis, in the process of amyloid protein aggregation, in the mechanisms of interaction between the amyloid proteins and the cell membrane, and in the amyloid neurotoxicity [19–25].

In the outer leaflet of the actual neuronal membrane, the unsaturated palmitoyl, oleoyl-*sn*-phosphatidylcholine (POPC) and Chol are abundant, and GM1 ganglioside accounts for only 5–10% of the total lipids [26]. Conversely, GM1 ganglioside is abundant in lipid-rafts, is representative of ganglioside distribution and known as the most popular raft-marker [27–29]. It contains four neutral sugar moieties and a negatively charged sialic acid residue and is negative at physiologic pH [30].

Recently, GM1 has been indicated to play a key-role in the interaction between amyloid proteins and cellular membranes. It has been shown that GM1 is involved in Aβ formation through binding to several Aβ aggregates [31–34]. Ikeda et al. proposed in 2011 that GM1 clusters in lipid-rafts mediate the formation of toxic amyloid fibrils at the membrane surface [35]. Matsubara et al. reported that GM1 density is a crucial factor for the assembly of Aβ-protein on detergent-resistant membrane microdomain fraction of synaptic plasma membranes prepared from aged mouse brain. The authors found that high-density GM1 in nanoclusters was formed in the synaptosomal membrane and closely connected with the formation of the spherical Aβ aggregates. Therefore, they suggested that there would be a critical density of GM1 in nanoclusters to induce ganglioside-Aβ binding, acting as an endogenous seed for Aβ assembly in Alzheimer's disease brains [36].

In Molecular Dynamics (MD) simulations of the behaviour of Aβ molecules interacting with GM1 containing raft-like membrane, the oligosaccharide head-group of GM1 was observed to play a crucial role in the peptide binding. Manna and Mukhopadhyay have simulated three different model membranes composed of POPC, Chol/POPC, and GM1/Chol/POPC, concluding that the carbohydrate head-group of GM1, located outside the lipid bilayers, acted as binding site for Aβ [37].

The role-played by Chol in the interaction Aβ-GM1 has been also investigated using a combination of biophysical and MD approaches. Fantini et al. showed that Chol accelerates the protein aggregation, and that Aβ is bound to the apolar phase of the membrane by sugar-aromatic interactions between the glycone part of the GM1 and specific amino acid side chains in the protein [38].

Notably, the fundamental role played by GM1 has been also demonstrated for other amyloid proteins. As an example, Botto et al. investigated prion/ganglioside relationship in a neuronal cellular model, i.e. cerebellar granule cells. They concluded that prion-GM1 interaction at the cell surface could play a significant role in the

mechanism predisposing to pathology [39]. Bucciantini et al. showed that yeast prion Sup35 fibril binding and toxicity were affected by GM1. They observed the complete inhibition of binding and toxicity after the cutting of sialic acid moiety by neuraminidase [40].

Remarkably, a similar effect has been reported by some of us also for the salmon calcitonin (sCT). In our study, we found that sCT is toxic for mature primary hippocampal neurons and that the lipid-raft disruption, obtained by neuraminidase, protects against toxicity [41].

sCT can be a useful probe to investigate the interaction between amyloid proteins and a lipid membrane models. Calcitonins are polypeptide hormones with 32 amino acids implicated in Ca home-ostasis [42]. sCT aggregation, which has been widely studied, is typical of amyloid proteins [43] but is characterized by a very slow aggregation rate and this peculiarity is at the basis of its pharmacological use [25]. Due to its pK=10.4, this protein is positive at physiologic pH. Schubert et al. firstly showed that human CT was toxic to cells in culture [9], while, Wang et al. showed the same for bovine CT [44]. More recently, we showed that sCT oligomers were toxic to mature primary neurons and, we reported the evidence of sCT "pore-like" structure oligomers, that is very similar to those described for other amyloid proteins and in particular for Aβ. Noticeably, these structures form Ca^{2+}-permeable pores when inserted into rafts-containing liposomes. We demonstrated that the presence of lipid-rafts in liposomes strongly favours the binding of sCT with a consequent increase of its β-secondary structure content. Conversely, sCT slightly interacts with raft-free liposomes, without any significant conformational modification [4,41,45,46].

However, despite the proliferation of studies on the interaction of amyloid proteins with lipid-raft, still little is known about the involved molecular mechanisms, and whether a specific molecule in the rafts triggers the binding and the following structural arrangement of the proteins. That is the reason why we decided to develop simplified models of a lipid membrane mimicking the occurrence of lipid-rafts and to study their interaction with sCT.

The use of model membrane systems has remarkably improved the knowledge on the biochemistry of amyloid proteins interacting with lipids [17]. Although very simplified compared to the complexity of biological cell membranes, lipid bilayers and monolayers can be employed as useful models. On one hand, liposomes can be easily prepared and are the most used bilayer model. On the other hand, the Langmuir technique allows preparing monomolecular films at the air-water interface that have been successfully used for the study of the phase behaviour of lipid systems.

Simplified models for lipid-rafts were proposed, based on the observation that detergent-resistant membranes obtained from actual cellular membranes were rich in sphingolipids and Chol and depleted in unsaturated phosphatidylcholines. Moreover, biophysical studies indicated that liposomes formulated with sphingolipids and Chol in ordered phases, such as L_o or solid-ordered (S_o), were found to be resistant to solubilisation with Triton X-100, while soluble if in L_e. GM1/Chol/POPC mixtures mimicking the local composition of lipid-rafts in the cellular membrane are presently used as raft models [37,38].

Langmuir monolayer technique is a potent tool providing information about the interactions involved, miscibility and stability of the monolayer. Thermodynamic measurements provide insights on the lipid mosaic phase and its modification due to the presence of proteins (i.e. binding, aggregation and/or mixing) [47–52]. The thermodynamics of the interaction is usually investigated by depositing at the air-subphase interface premixed mixtures of the peptide with the membrane models, at increasing molar ratios [53–59]. The surface pressure isotherms provide useful information on the nature of the short-range and long-range interactions between the molecules, especially between lipids and Aβ peptides [59,60]. The two-dimensional Langmuir film morphology at the water-air interface can be visualized, in real time and with a low resolution (few microns), using Brewster Angle Microscopy (BAM). This technique is sensitive to the changes in

the optical parameters of the monolayer, and the local changes in packing or orientation of the molecules are easily monitored [61]. Recently, BAM has been successfully applied in the study of the formation of protein clusters in model membranes constituted by binary lipid mixtures [62].

The Langmuir monolayers can be successfully deposited onto atomically flat surfaces, accurately controlling the surface pressure, to prepare solid monolayers (Langmuir-Blodgett technique). Depending on the hydrophobicity of the employed substrate and the deposition procedure, it is possible to prepare double layers mimicking the lipid component of actual membranes. During the deposition, the water is kept out of the lipid bilayer and, if we are in compact phase such as liquid-condensed (L_c) or L_o, the arrangement is enough rigid to avoid dramatic collapses. That is the reason why, for a high-resolution investigation of the Langmuir-Blodgett (L-B) film in air, Tapping Mode-Atomic Force Microscopy (TM-AFM) has be successfully used [63]. This technique was able to obtain molecular lateral resolution and subnanometer vertical resolution, yielding molecular-scale topographic maps of surfaces.

Here we prepared, by the L-B technique, a simplified model of the neuronal membrane. More in particular, we prepared an outer monolayer mimicking the local composition of lipid-raft characterized by a high content of GM1 and a minority part of Chol and POPC (0.50/0.25/0.25) [37]. This monolayer was deposited onto mica covered by a pure POPC monolayer simulating the inner leaflet of the lipid bilayer. The deposition surface pressure of both monolayers was kept constant at 22 mN/m, allowing us to consider the whole bilayer to be in L_c phase [64,65]. This is valid for the whole model but the local lipid arrangement in the outer leaflet, rich in saturated GM1, can be in the L_o phase that characterizes lipid-rafts.

We prepared and studied in-air and at molecular resolution by TM-AFM the outer monolayer with embedded sCT at a concentration such that the number of proteins equals that of GM1. Moreover, to understand the nature of the interaction between sCT and our model membrane we prepared and studied by Laser Doppler electrophoresis, the ζ-potential of GM1/Chol/POPC liposomes of lipid composition as the outer monolayers of the model discussed before (0.50/0.25/0.25).

Finally, to further investigate the interaction thermodynamic of sCT with the outer leaflet of our model, Langmuir monolayers deposited at the air-water interface and containing increasing sCT percentages, were prepared and studied by combined experiments of compression isotherms and Brewster Angle Microscopy (BAM).

2. Materials and methods

2.1. Materials

1-Palmitoyl-2-oleoyl-*sn*-phosphatydilhcoline (POPC), (Molecular weight: 760.08) and monosialoganglioside-GM1 (Molecular weight: 1545) from bovine brain and Chol (Molecular weight: 386.66) were purchased from SIGMA (SIGMA Chemical, St Louis, MO). Lyophilized sCT (Molecular weight: 3432) was purchased from European PHARMACOPOEIA (EDQM, Strasbourg, France) and stored at −18 °C before use. Chloroform, methanol, and other solvents were also purchased from SIGMA. Stock solution of POPC was prepared in chloroform (1 mg/ml). sCT was dissolved in 4:1 (v/v) chloroform/methanol containing 0.5% amyl alcohol. All the chemicals were used without further purification. Phosphate Buffered Saline (PBS, pH 7.4, I 0.16) was used. In all experiments and for cleaning procedures only ultra-pure MILLI-Q water was used. The composition of lipid-rafts was simulated using different mixtures of GM1, Chol and POPC. Chol and POPC were dissolved in chloroform and GM1 in 2:1:0.15 (v/v) chloroform/methanol/water. All used concentrations were 1 mg/ml. These solutions were mixed in appropriate ratios to form the different model membranes: i.e. GM1/Chol/POPC molar ratios 0.50/0.25/0.25: Chol/POPC 0.50/0.50 molar ratio. sCT was added to the lipid mixture

before the Langmuir film preparations.

2.2. Langmuir and Langmuir-Blodgett monolayer preparation and characterization

Langmuir monolayers were prepared using a KSV3000 Langmuir trough with a total area of 79.5×10^2 mm^2 (KSV LTD, Finland), placed on an anti-vibration table and enclosed in a Plexiglas box to avoid contamination and dust deposition. All the experiments were performed using a trough thermostated by a water-bath circulator at a temperature of (20 ± 0.1 °C). The Langmuir monolayers were spread on PBS (0.15 M) subphases at pH 7.4. Such a subphase was chosen after a large number of experiments aimed at achieving a good film stability and optimal reproducibility.

The films were characterized by surface pressure-area (π-A) isotherms studies. Compression was achieved with the symmetric movement of the two barriers. Trough and barriers were thoroughly cleaned with appropriate solvents. Prior to film deposition, the surface was cleaned repeatedly by sweeping the barriers and aspirating the surface in between, until no change in surface pressure was detectable compared to the closed and the open positions. The surface pressure during the film compression was monitored using a microbalance and a Wilhelmy plate. Appropriate amounts of the lipid solution (80–120 µl) were spread in a drop-wise manner with a 10-µl microsyringe. Monolayers were compressed at a rate of 30 cm^2/min. Before starting the regular compression run, three successive compression/expansion cycles spanning the L_e phase of the monolayer, were performed to check monolayers stability and to verify the absence of hysteresis. For each film composition at least three isotherms were carried out in identical conditions to ensure reproducibility. The representative isotherm at each molar ratio was obtained by averaging, over the x-axis, at least tree reproducible isotherms.

Selected samples were deposited onto freshly cleaved mica to obtain a L-B film to be studied by AFM. Two kind of L-B films were prepared: i) plain POPC onto mica simulating the inner membrane leaflet and used as substrate of the outer monolayer; ii) GM1/Chol/POPC molar ratios 0.50/0.25/0.25 simulating lipid-raft in the outer membrane leaflet and containing sCT at X=0.34 molar ratio.

The plain POPC monolayer was deposited by vertically extracting the mica sheet through the film at a constant rate of 0.1 mm/min and keeping film surface tension constant at 22 mN/m. The mica had been previously half-dipped into the subphase before monolayer deposition. This hydrophobic L-B film was used as substrate for the deposition of the L-B monolayer simulating the lipid-raft with sCT. Due to the POPC monolayer hydrophobicity, the deposition was performed by dipping it into the subphase, keeping the film surface tension constant at 22 mN/m.

Supported L-B monolayers were stored in a dry atmosphere to keep them stable over a long period of time. Five series of samples were prepared and the best three series were chosen for the experiments.

2.3. Atomic Force Microscopy (AFM)

Images were collected in air, at room temperature using a DIMENSION ICON with a Nanoscope V Controller (Brucker AXS, Germany). The tapping mode was employed, using etched silicon cantilever probes of 125 µm nominal length, at a drive frequency of ~300 kHz. Both height and phase data were recorded at a scan rate of 1 Hz and stored in a 512×512−pixel format. Images were processed using Gwiddion software. For those used in the measurements of the heights, the only image processing was zero order flattering. The only other image adjustments were setting the image heights range, colour contrast, and colour offset for best appearance of structural details. we used AFM in contact mode to measure the layer heights by scratching the soft lipid films up to the hard mica.

2.4. Brewster Angle Microscopy (BAM)

BAM is a technique that allows for the direct visualization of Langmuir films at the air-water interface and is based on the principle that p-polarized light is not reflected at the Brewster angle. The presence of a monolayer results in the reflection of light with the consequent image formation. A Brewster angle microscope BAM 2 plus NFT (NFT Gottingen, Germany), mounted on the KSV3000 Langmuir trough (KSV, Helsinki, Finland), is used to capture images during the formation and compression of the films, at desired target surface pressure (the lateral resolution can be estimated to be in the order of 3 μm). The trough and the microscope were both housed in a cabinet to avoid air currents. The images were digitized using a frame grabber and treated with image-processing software to correct both distortions resulting from the observation at the Brewster angle and inhomogeneity in the laser illumination.

2.5. Thermodynamic analysis of Langmuir mixed-monolayers

We have analysed the measured Langmuir isotherms in terms of mean molecular areas and excess energy of mixing at selected lateral pressures. The way in which the mean molecular areas depend on the composition of the mixed monolayer gives information on possible interactions between the different molecular species in the film [52]. In the "area analysis", a linear dependence indicates either an ideal mixing or a complete immiscibility of the two components. Conversely, while repulsive interactions cause positive deviations from linearity, negative deviations indicate attractive interactions between the different molecular species [66,67]. The "partial molecular area" relative to sCT can be also defined as the variation of the total monololayer area occurring when X increases. This parameter can be evaluated by the classical"-method of the tangents" applied to the "area-analysis" results [52].

The excess free energy of mixing, ΔG, was calculated from the (π-A) isotherms of the mixed monolayer, by the method developed by Goodrich:

$$\Delta G = \int_0^\pi A_{1,2} d\pi - X_1 \int_0^\pi A_1 d\pi - X_2 \int_0^\pi A_2 d\pi \qquad (1)$$

where X is the molar fraction, with subscripts **1** and **2** referring to the two components (in our case 1 is referred to the lipid mixture and 2 to sCT) and subscript **1,2** to their mixture $(X_1 + X_2 = 1)$. The excess free energy of mixing provides information on whether the mixing is energetically favoured (ΔG < 0), or not (ΔG > 0), compared to an ideal mixing (ΔG=0) for which it is assumed that the interactions of a molecule with the molecules of the other species, or with the molecule of its own species, are equal. Actually, ΔG < 0 indicates that the interaction between the two different components is favoured, whereas ΔG > 0 can be interpreted as a tendency of the molecules to interact preferentially with molecules of the same kind, thus, suggesting a phase separation or an aggregation of one component [52,57]. In order to estimate the error on ΔG, we have used the formula:

$$Error \Delta G = \sqrt{(\Delta S_{1,2})^2 + (X_1 \Delta S_1)^2 + (X_2 \Delta S_2)^2} \qquad (2)$$

where: $\Delta S_{1,2}$, ΔS_1 and ΔS_2 are the standard errors associated to the mean of the value of integrals (named $S_{1,2}$, S_1 and S_2) in Eq. (1), calculated at the different surface pressure π, for the single reproducible isotherms.

2.6. Liposome preparation

As in the case of Langmuir films, the composition of lipid-rafts was simulated using different mixtures of GM1, Chol and POPC. Chol and POPC were dissolved in chloroform and GM1 in 2:1:0.15 (v/v) chloroform/methanol/water. All used concentrations were 1 mg/ml. These solutions were mixed to simulate the raft model with GM1/Chol/POPC molar ratios 0.50/0.25/0.25. sCT, dissolved in 4:1 (v/v)

chloroform/methanol containing 0.5% amyl alcohol, was added to the raft simulating solution before the liposome extrusion, at a final molar fraction of 0.34. Two control liposomes were also prepared, that is plain POPC and Chol/POPC. The aqueous dispersions of liposomes were prepared in PBS (0.15 M), according to the extrusion technique associated with the freeze-thaw protocol, as described in the literature [68,69]. Briefly, a film of lipid was prepared by evaporation of the solution containing the appropriate amount of lipids and protein to obtain a dispersion of multilamellar vesicles (MLV). PBS buffer solution (Aldrich, 10−2 M, pH 7.4) was added to obtain lipid dispersions at a final concentration of 1 mg/ml. The solutions were vortex-mixed and freeze-thawed 6× from liquid nitrogen to 307 K. Dispersions were then extruded through a polycarbonate membrane with pores of 100 nm (10×) at 307 K using a 2.5 ml extruder (Lipex Biomembranes, Vancouver, Canada).

2.7. ζ-potential and size measurements by Dynamic Light Scattering (DLS)

Both the electrophoretic mobility and the size of liposomes were measured by means of an integrated apparatus, NanoZeta-Sizer (Malvern Instruments Ltd., UK), equipped with a 5 mW He–Ne laser. The normalized intensity autocorrelation functions were measured at an angle of 173°. The autocorrelation functions were analysed by using the NNLS algorithm [70]. The decay times were used to obtain the distribution of the diffusion coefficients D of the particles, further converted into a distribution of the effective hydrodynamic radii, R_H, using the Stokes- Einstein relationship $R_H = k_B T/6\pi\eta D$, where $k_B T$ is the thermal energy and η the solvent viscosity. The values of the radii reported here correspond to the average on the "intensity weighted" distribution [71].

The particles ζ-potential was obtained from the electrophoretic mobility μ measured by combining laser Doppler velocimetry (LDV) and phase analysis light scattering (PALS) [72], thus allowing an accurate determination of the average mobility and of the mobility distribution. The mobility μ was converted into the ζ potential using the Smoluchowski relation ζ=μ η/ε, where η and ε are the viscosity and the permittivity of the solvent phase, respectively.

3. Results and discussion

3.1. Atomic Force Microscopy (AFM)

In our study, we have investigated the interaction of the amyloid sCT with a model system that simulates the lipid components of a neuronal cellular membrane. Two L-B monolayers were prepared and deposited in the L_c phase (π=22 mN/m), because the equivalence between the physical properties of mono- and bilayers has been studied and identified when they are in the L_c phase [65].

The lower monolayer is composed of pure unsaturated POPC lipid, directly deposited onto mica, while the external deposited on the first, by the GM1/Chol/POPC mixture (0.5/0.25/0.25) and sCT.

The external layer simulates the local composition of lipid-rafts present in the outer neuronal membrane leaflet. We note that this is a model of the lipid component of the raft and not of the whole outer membrane leaflet that in the actual membrane is characterized by a low GM1 content and an high concentration of membrane proteins.

We added to the outer monolayer sCT before the deposition at the air-water interface, at a concentration such that the number of protein molecules equals that of GM1 (X=0.34). This choice and not to insert sCT in the water subphase, was motivated by the possibility of controlling the exact relative sCT-GM1 molar ratio. The addiction of sCT to the subphase would lead to indeterminations in the exact evaluation of the amount of protein actually adsorbed in the monolayer.

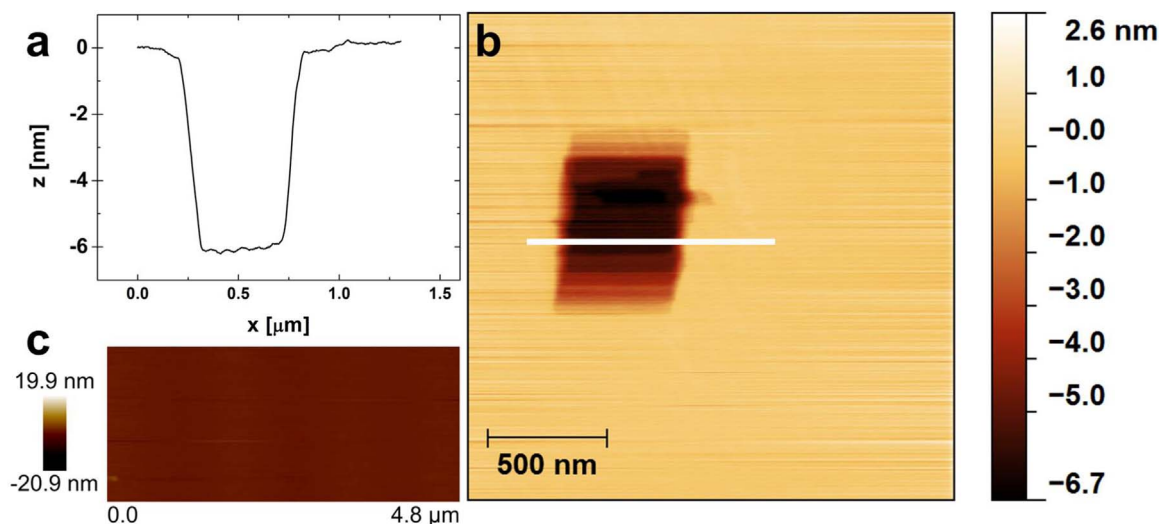For a preliminary control of the correct formation of the lipid

Fig. 1. AFM study of the model made of a Chol/POPC (0.5/0.5) layer deposited onto mica covered by POPC. Fig. 1a shows the line-profile obtained after the scratching performed in contact mode (white line in Fig. 1b). Fig. 1c shows the same sample before the scratching, imaged in TM-AFM. A flat surface can be observed.

bilayers and the absence of dramatic dehydration phenomena, we studied the simple Chol/POPC (0.5/0.5) layer without sCT, deposited onto POPC on mica. A certain region of the film, imaged by TM-AFM, was also scratched by contact-mode AFM, thus allowing the determination of the thickness. Results are reported in Fig. 1. As expected, TM-AFM images revealed a very flat surface (Fig. 1c), without holes or islands and the line profile (Fig. 1a) relative to the scratched region (Fig. 1b) showed a hole of about 6 nm deep, in good agreement with the known dimension of a POPC bilayer.

This control clearly demonstrates that our bilayer preparation method correctly leads to homogeneous lipid membrane models, not dramatically affected by dehydration phenomena that could collapse their structure. This can be explained considering that the deposition performed by the L-B technique allowed us to accurately maintain constant the pressure at 22 mN/m while the hydrophilic POPC heads were transferred to the hydrophilic, atomically flat mica (inner monolayer). At the same time, during the outer bilayer deposition the hydrophobic tails of the Langmuir film were transferred to the hydrophobic tails of the first POPC monolayer (outer monolayer). Thus, when the bilayer is formed, water can be localized only outside the hydrophobic backbone and the lipid structure, in the L_c phase is enough compact to stabilize the bilayer.

Fig. 2 shows TM-AFM images relative to independent samples representative of the model containing GM1 and sCT. As it can be observed a very flat dark surface appears in both samples, together with flat islands of about 1.5 nm high. The percentage of surface covered by these islands changes in the various zones of the same sample and between the samples. Fig. 2a shows a zone with few islands, while in Fig. 2c the highest surface (light brown) is more extended. The height difference between the two kinds of surfaces is about 1.5 nm, compatible with the different heights of POPC and GM1 molecules.

Notably, a characteristic feature can be identified in all situations, that is globular bright aggregates localized exclusively onto the highest surface. These aggregates are generally globules of varying heights, ranging from few to hundred nanometers. Higher is the aggregate bigger is its diameter. Rod-like aggregates can be also found seldom (Fig. 2d) that can be interpreted as early-formed sCT protofibrils as reported in literature [11].

TM-AFM images relative to the sCT-free control model (GM1/Chol/POPC) revealed the same two flat surfaces described before. Notably, the features localized onto the high surfaces were totally absent (data not shown). Thus, we speculate that these structures can be interpreted as formed by sCT aggregates of different sizes.

Interestingly, Matsubara et al. described similar structures in a

AFM study, interpreted as due to the formation of spherical Aβ-protein aggregates driven by high-density of GM1 localized in synaptosomes [36]. As further support of the similarity between the aggregates observed by Matsubara et al. and the one observed in our investigation, we note that the adopted preparation protocol for the bilayer model system is the same, i.e. an inner POPC layer deposited on mica and an outer GM1 rich layer deposited above.

The all body of our AFM study indicates that stable double layers were formed onto atomically flat mica and that the outer surface was characterized by islands, more or less extended, of heights compatible with the occurrence of GM1 molecules. Globules that can be identified as sCT aggregates of different sizes, were observed only onto these islands.

3.2. Thermodynamic of the interaction of sCT with the outer leaflet

To better investigate the interaction between the amyloid sCT with the outer leaflet of our model mimicking the lipid component of the external leaflet of a neuronal membrane, we studied by compression isotherms Langmuir monolayers made of GM1/Chol/POPC (0.50/0.25/0.25) with sCT at increasing molar ratios. The protein was added to the lipid mixtures before the monolayer deposition.

Fig. 3a shows the (π-A) isotherms of 8 monolayers, the black full-line curve being that of the plain GM1/Chol/POPC mixture, the dashed line corresponding to sCT, and the remaining 6 isotherms to the mixtures at increasing sCT molar fractions, from 0.20 to 0.80.

As expected, the sCT isotherm is located at the highest mean molecular area (MMA) values, characterized by a pronounced knee, at approximately 400 Å^2 and 18 mN/m, in agreement with previous observations [73,74]. In a detailed study, Romeu et al. demonstrated that this knee and the following zone of an increased compressibility can been attributed to a film instability. Based on the hysteresis behaviour the authors concluded that sCTs adopt a close-packed form before the plateau, with only solvated polar aminoacids submerged in the subphase. At the plateau, described as a collapse, they proposed that the progressive reconfiguration of each molecule as a chain of loops suspended from less polar units occurs. Thus the protein, due to its water solubility, was expelled from the monolayer with most of the polar amino acids submerged in the subphase.

However, in the same study, the authors indicated that the film is stable if compressed up to surface tensions before collapse (π < 18 mN/m), and that there is not solubility of molecules from the monolayer under these conditions [74].

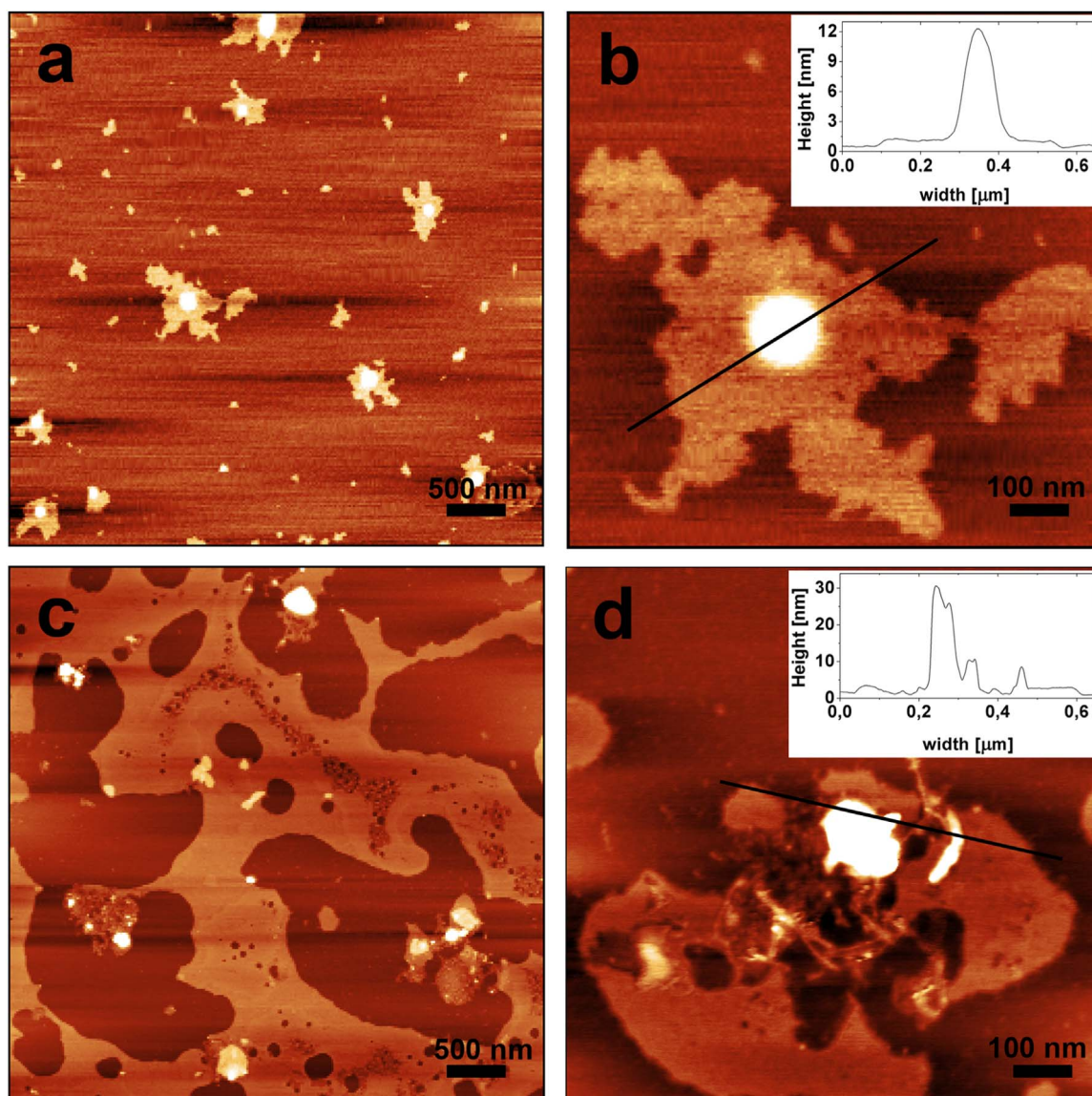For what concerns the lipid component, it is worth noting that the

Fig. 2. AFM images relative to the raft model made of GM1/Chol/POPC (0.50/0.25/0.25) and sCT, deposited onto mica covered by plain POPC. sCT was added before the deposition to the outer monolayer at X=0.34 molar fraction. Fig. 2a shows a wide field, with many repeated features magnified in Fig. 2b. The inset represents the line-profile of the zone indicated in Fig. 2b. Fig. 2c and d are relative to an independent sample.

GM1/POPC/Chol isotherm shows a collapse pressure of about 63 mN/m and an evident inflection between 45 and 50 mN/m. The last feature can be attributed to the occurrence of an L_c-L_o phase transition.

The typical sCT knee characterizes all isotherms of the mixtures. The feature due to the L_c-L_o phase transition is still present, shifted depending on the sCT molar fraction, and the collapse pressures tend to the sCT-free one. This suggests that the film behaviour strongly depends from the lipid matrix.

Fig. 3b shows the "area-analysis". Notably, if the analysis is performed for pressures above the sCT knee (20 and 25 mN/m) the curves remain almost linear while, when the analysis is performed for pressures below the knee (5, 10 and 15 mN/m), the measured MMA shows a non-linear behaviour or better, a piecewise linear behaviour. The slope change occurs around X=0.34 sCT molar ratio. Apparently, above this threshold the presence of sCT molecules in excess affects only marginally the MMA values and a plateau appears, up to 0.6 molar ratio. A possible interpretation of this plateau is that, in this concentration range and at these low pressures, part of the sCT molecules were expelled from the monolayer.

Fig. 4 shows the sCT "partial molecular area" (in red) calculated in

two representative cases, which is above and below the sCT knee (π=18 mN/m). As in the "area-analysis", there is a marked deviation from the linearity when we are below the knee (a). The sCT partial molecular area (in red) reaches a minimum between 0.34 and 0.5, supporting our idea that some sCT molecules were expelled from the monolayer beyond X > 0.34.

The same analysis, performed at pressures higher than the sCT knee (b), shows that the sCT partial molecular area is practically constant (in red). This suggests that, at this pressure some sCTs are embedded in the monolayer, independently from X, and that the proteins in excess are located outside.

Finally, the inset of Fig. 3a shows the "ΔG-analysis" results of our system and, as discussed by Romeu et al. [73,74], can be considered "quantitative" only for pressures less than the sCT knee (5, 15 mN/m). ΔG grows up to a 0.34 sCT molar fraction, reaching a maximum (about 3 KJ/m), suggesting that, up this molar fraction, a protein aggregation occurred in the monolayer.

Notably, this value corresponds to the beginning of the plateau in the "area-analysis" results. Then, ΔG decreases and remains close to zero up to 0.60 molar fraction, where the plateau of the MMA ends.
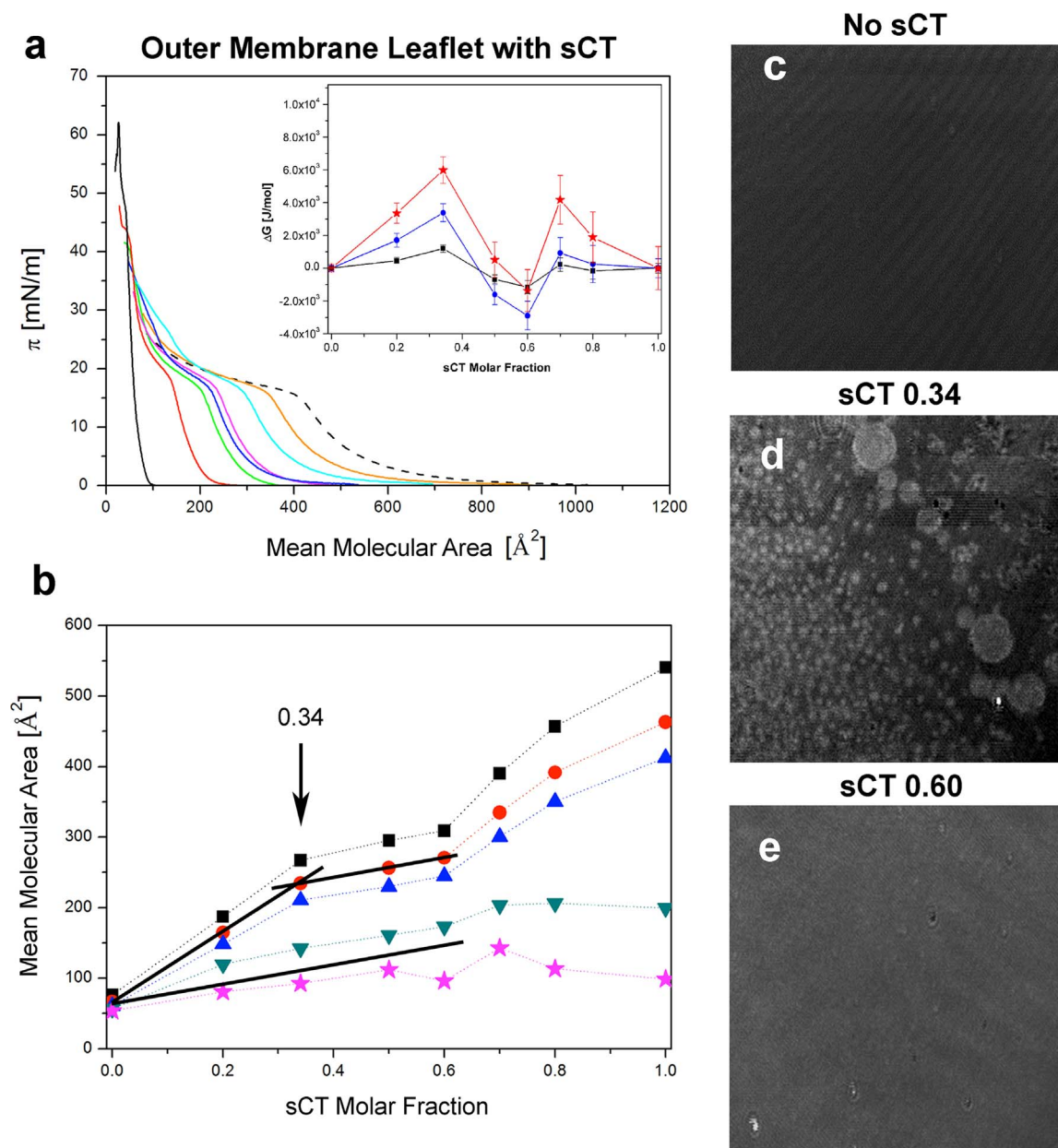
Fig. 3. Compression isotherms and BAM images (frame of 1×1 mm) relative to the model of the outer membrane leaflet: GM1/Chol/POPC and sCT. Fig. 3a shows isotherms relative to GM1/Chol/POPC (black solid) and sCT (dashed) at different molar ratios: 0.20 (red), 0.34 (green), 0.50 (blue), 0.60 (pink), 0.70 (light-blue), 0.80 (orange). Fig. 3b shows the "area-analysis" of this system at five surface pressures: ■ π=5 mN/m, • π=10 mN/m, ▲ π=15 mN/m, ▼ π=20 mN/m, ★ π=25 mN/m. Errors are within the symbols. The inset of Fig. 3a shows the "ΔG-analysis" at three surface pressures: ■ π=5 mN/m, • π=15 mN/m, ★ π=25 mN/m. BAM images show the monolayer morphology (in the L_c phase at π=22 mN/m) observed without sCT (Fig. 3c), with sCT at 0.34 (Fig. 3d) and at 0.60 (Fig. 3e) molar fraction.

For X > 0.6, the MMA (Fig. 3b) return to a linear behaviour that is the film pressure is affected by the sCT presence. This suggests that in this range the film structure totally changed and was determined by the big and abundant sCT molecules retained in the monolayer.

For what concerns BAM images, results relative to the GM1/POPC/Chol plain mixture didn't show any defined structure (Fig. 3c). The film appeared as a single L_c homogeneous phase due to the abundant saturated GM1 chains, in good agreement with the relative isotherm.

Conversely, the image relative to 0.34 molar ratio shows, for the first time, well-defined white structures (of about 6 μm) together with larger islands of about 15–100 μm diameters (Fig. 3d). This finding is quite interesting because, under this condition, a system change was indicated by "area-analysis", "partial molecular area-analysis" and "ΔG-analysis".

Finally, BAM images relative to 0.60 molar fraction (Fig. 3e) do not show any white features but only a grey homogeneous phase. We speculate that this is due to a thicker monolayer formed by the big and abundant sCT molecules, embedded in the monolayer. Indeed, BAM is a technique where images of enhanced brightness are formed by structures protruding from the monolayer, due to quadratic dependence of the reflectance with the thickness [75].

To better shed light on the role played by GM1 in the interaction of sCT with the outer leaflet of our membrane model, we prepared and studied GM1-free Langmuir films made of Chol/POPC. As before, we added protein molecules at increasing molar ratios, from 0.20 to 0.80. Fig. 5a shows the resulting (π-A) isotherms.

The collapse pressure of the plain Chol/POPC film is around 50 mN/m, lower than the value observed in the presence of GM1. Interestingly, the feature we attributed to the L_c-L_o phase transition in the isotherm of GM1/POPC/Chol mixture is now totally absent and this
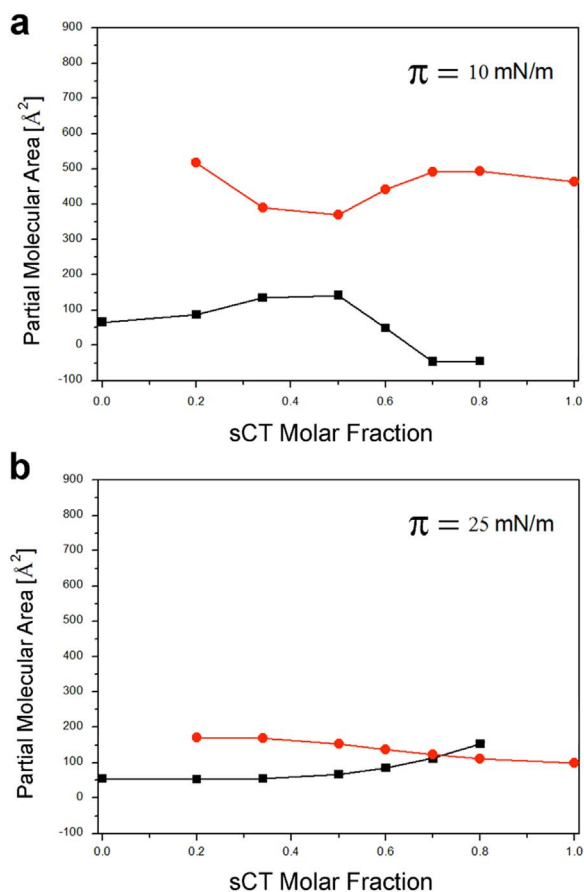
Fig. 4. Partial molecular area results relative to the to the model of the outer membrane leaflet made of GM1/Chol/POPC and sCT. Symbols • indicate data relative to sCT while ■ to the GM1/Chol/POPC matrix. The analysis has been performed at π=10 mN/m (a) and π=25 mN/m (b), which is above and below the sCT knee (π=18 mN/m).

confirms that the L_o phase was due to the presence of GM1.

As expected, the presence of sCT molecules induces the typical sCT knee. The "area-analysis" reported in Fig. 5b shows linear behaviours at all pressures, above and below the sCT knee, and the plateau observed in the presence of GM1 don't appear. The inset of Fig. 4a shows the "ΔG-analysis". Quantitative results for 5 and 15 mN/m (< 18 mN/m) indicate a flat trend characterized by positive values (< 2 KJ/m).

This finding demonstrates that the presence of GM1 was responsible for the highest ΔG values measured before (see the inset of Fig. 3a).

In conclusion, all our thermodynamic results indicate that there was an interaction between sCT and the monolayer mimicking the lipid component of the outer leaflet, triggered by the presence of GM1.

Notably, the system had a change beyond X=0.34. It is important to note that, at X=0.34 the number of sCT molecules equals that of GM1 molecules (50% of 0.66 molar fraction).

3.3. ζ-potential and size experiments

To investigate the electrostatic nature of the interaction between sCT and model membranes, we prepared liposomes made of GM1/Chol/POPC, with the molar composition of the outer L-B monolayer previously described (0.5/0.25/0.25) and with sCT at a molar fraction X=0.34. Our working hypothesis is that the sCT, which is positively charged in PBS at pH 7.3, is able to bind to the negatively charged sialic acid moiety of GM1, located at the liposome surface [30].

To clarify if two different protocols of addition of the protein change the interaction mechanisms between sCT and GM1, we performed our
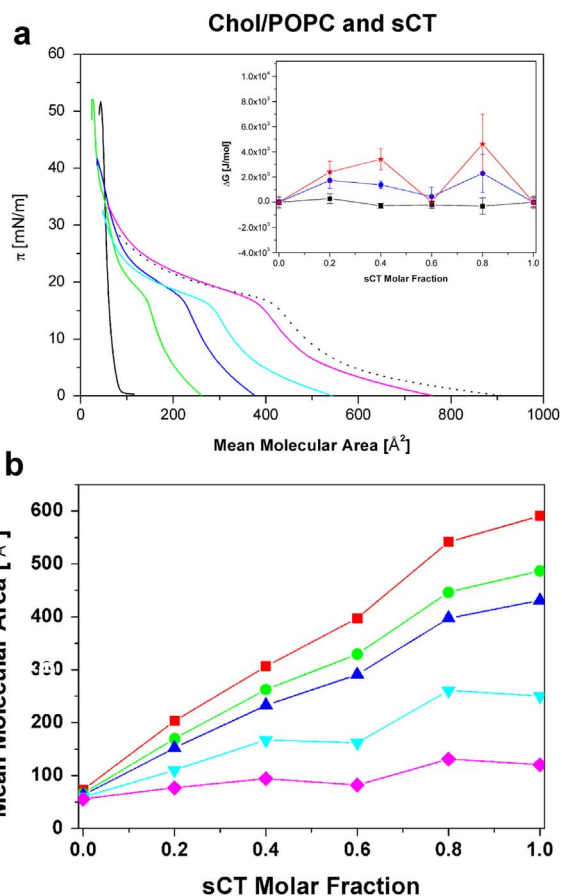

Fig. 5. Compression isotherms relative to the GM1-free control model made of Chol/POPC and sCT. Fig. 5a shows the isotherms of plain lipids (black solid) and sCT (dashed) at different molar ratios: 0.20 (green), 0.40 (blue), 0.60 (light-blue) and 0.80 (pink) for Chol/POPC. Fig. 5b shows the "area-analysis" of this system at five surface pressures: ■ π=5 mN/m, • π=10 mN/m, ▲ π=15 mN/m, ▼ π=20 mN/m, ★ π=25 mN/m. Errors are within the symbols. The inset of Fig. 5a shows the "ΔG-analysis" at three surface pressures: ■ π=5 mN/m, • π=15 mN/m, ★ π=25 mN/m.

experiments on liposomes prepared in two ways: i) by a co-dispersion of sCT and lipids in the organic solvent before the liposome preparation; ii) by adding sCT to the aqueous medium where liposomes were preformed.

The values of ζ-potential obtained from electrophoresis on the different liposome formulations are summarized in Table 1, together with the corresponding average hydrodynamic radius and peak half-width determined by DLS measurements.

It has to be noted that the measured radii of all the liposomes are in the same range. The homogeneity of the dispersions allows us to rule out that ζ-potential measurements were influenced by the possible change of the total liposome surface due to radius variations.

Notably, in the absence of sCT the ζ-potential of GM1/Chol/POPC liposomes is remarkably negative (i.e. −14/−15 mV), and doesn't depend from the liposome concentration, as it can be observed comparing the values with those of the diluted sample.

When sCT is mixed to lipids during the liposome preparation, the ζ-potential values of GM1/Chol/POPC+sCT liposomes is less negative with respect to pure GM1/Chol/POPC liposomes, demonstrating the positive contribution furnished by the presence of the protein. Moreover, when sCT is added to the preformed GM1/Chol/POPC liposomes, the value of the ζ-potential is even further reduced, indicating that the protein is able to effectively adsorb at the liposome surface, neutralizing in part the negative charge.

As shown in Fig. 6a, the presence of an sCT coating is further suggested by the radius of sCT-liposome complex (about 80 nm),

Table 1

ζ-potential, mean hydrodynamic radius R and peak half-width of the size distribution of liposomes with different composition. In GM1/Chol/POPC+sCT samples two populations with different size are present, as indicated in relative columns. The hydrodynamic radius R and the peak half-width or standard deviation, indicative of the distribution in the peak, is calculated directly from the size histograms, obtained from NNLS intensity weighted distribution analysis of DLS data. Errors on data are the statistical errors on three different repeated measurements, each one composed on a set of 15 submeasurements, at least.

| Sample	ζ-potential [mV]	R [nm]	Peak half-width [nm]
GM1/Chol/POPC	−14.0 ± 1.4	60 ± 1.7	20 ± 1.1
GM1/Chol/POPC (diluted 1–5 in PBS)	−15.6 ± 1.5	58 ± 2.1	25 ± 1.7
GM1/Chol/POPC + sCT (co-dispersion)	−9.1 ± 0.9	79.7 ± 3.2 8.2 ± 0.5	31.5 ± 1.3 1.8 ± 0.3
GM1/Chol/POPC + sCT (added to liposome suspension in the PBS solution)	−5.1 ± 0.5	72.8 ± 2.5 11.1 ± 1.2	29.9 ± 1.2 3.1 ± 0.8
Chol/POPC	− 4.3 ± 0.4	80 ± 1.4	30 ± 1.8
Chol/POPC + sCT added to liposome suspension in the PBS solution	−3.8 ± 0.5	80 ± 3.5	32 ± 2.1
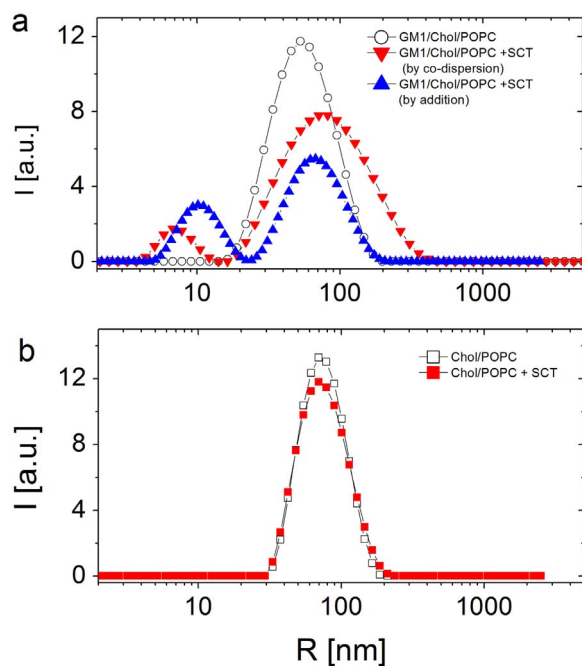
Fig. 6. DLS size distributions of the liposomal samples reported in Table 1, obtained from intensity-weighted NNLS analysis. For GM1/Chol/POPC liposomes (panel A, ○) the presence of sCT in the bilayer (▼, ▲) promotes the increase of mean hydrodynamic radius and the formation of smaller sCT aggregates, independently of the addition protocol. In Chol/POPC liposomes without GM1 (panel B, □), no difference in radius and size distribution is found after sCT addition (panel B, ■).

significantly larger than radius of bare liposomes (about 60 nm). Moreover, smaller objects with radius 8-11 nm were found when sCT was added, in both ways. We interpret this fact by the presence of sCT oligomers, free in solution, likely formed at the liposome surface because of the presence of GM1. The total absence of small aggregates in the sample Chol/POPC+sCT (see Table 1) indicates that the protein aggregation is triggered by the presence of GM1 at the liposome surface and that only undetectable sCT monomers, non-interacting with liposomes, were present free in solution.

To focus on the role-played by GM1, we also prepared GM1-free liposomes, made of Chol/POPC. In this system, the ζ-potential is slightly negative (i.e. −4 mV) and the external addition of the protein didn't alter this value, demonstrating that the protein didn't adsorb at the liposome surface.

As shown in Fig. 6b, the addition of the protein didn't affect the size of the liposomes, confirming that the sCT didn't form an external coating, as in the case of liposomes with GM1. The biggest size of Chol/POPC liposomes (about 80 nm) compared with the GM1/Chol/POPC one (about 60 nm) could be interpreted as due to the more compact structure of the bilayer induced by the presence of GM1, with its saturated tails. Our results strongly suggest that the positive sCT bound the negative GM1 moiety, thus shielding the negatively charged liposomes and resulting in quasi-neutral ζ-potential values. Notably, this is independent from the internal or external addition of sCT to liposomes.

3.4. The model

As discussed before, many studies have been conducted, both experimentally and theoretically, concerning the exact nature driving the interactions Aβ-GM1 but, up to now, the molecular mechanisms are not yet completely determined.

In a recent MD simulation performed with the GM1/POPC/Chol mixture, very similar to our experimental system, Manna and Mukhopadhyay suggested that the carbohydrate headgroup of GM1 acts as binding site for the amyloid protein [37]. Moreover, Fantini et al. showed by a Langmuir technique and MD combined study that also Chol actively participates to the binding of $A\beta_{1-16}$ with a GM1 dimer [38].

Up to now, no MD simulations for the interaction of sCT with GM1 have been performed and the studies cited before are Aβ-specific and can't be directly extrapolated to sCT, even if belonging to the amyloid family.

We speculate that a possible interpretation of the sCT binding to the GM1 can be based on the net charges of these two molecules. The polar and the positively charged aminoacids of the protein, in contact with the solvent at pH 7.4 can interact electrostatically with the negatively charged sialic acid moiety of GM1 [30].

In particular, the big sCT molecules having a volume of about 5 times the GM1, can bound to the GM1 polar head-groups and stabilized by Chol, according to the MD study of Fantini et al., [38] forming the complex sCT-GM1-Chol (see Fig. 7). This complex is characterized by the steric hindrance of the sCT and can be formed before the monolayer assembly.

After the monolayer formation, in L_c phase (π > 5 mN/m) [64,65], the molecules are vertically organized and the complexes can aggregate, forming an ordered L_o phase representing the skeleton of the raft and characterized by saturated tails (see Fig. 7a).

From our thermodynamic results, three situations can be imaged:

- when X < 0.34: the sCTs are less than GM1 molecules and the complexes sCT-GM1-Chol together with the GM1 in excess form an ordered phase constituting the raft (Fig. 7a);
- when X=0.34: the sCT number is equal to GM1 molecules. In this case, due to the lack of Chol there are sCTs in excess not forming the complex that can be expelled from the monolayer and can aggregate outside the monolayer (Fig. 7b);
- when X > 0.34: there are many sCT in excess and their aggregation proceeds forming spherical assembly on top of the raft, (Fig. 7c).

We note that, in this model, the whole monolayer can be in the L_c phase while the ordered GM1-rich domains in the L_o phase.

Our high-resolution AFM images of the membrane model in the L_c phase (π=22 mN/m) support this hypothesis, with the height difference between the two kinds of flat surfaces (about 1.5 nm) that can be attributed to the different dimensions of POPC and GM1 molecules (Fig. 7a) and the observed globules to sCT aggregates of different sizes
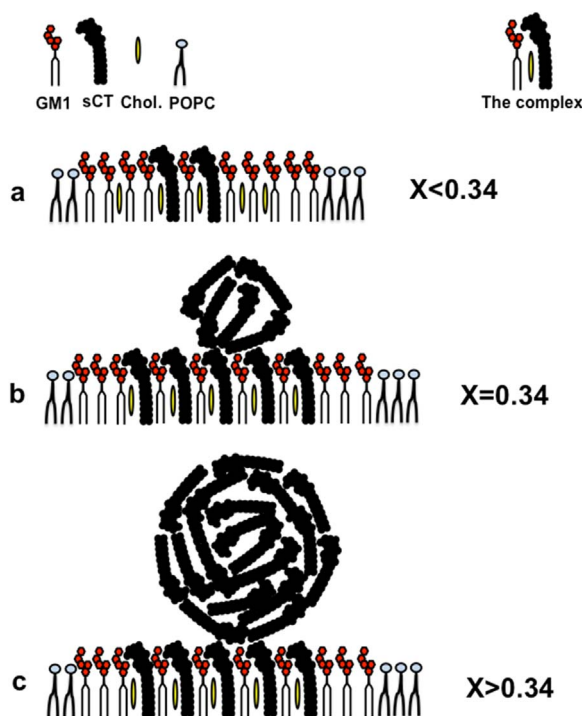
Fig. 7. Simplified graphical model of the possible interaction of the amyloid protein sCT molecules with the Langmuir monolayer simulating the raft containing outer neuronal membrane leaflet (0.50/0.25/0.25 molar fraction of GM1/Chol/POPC). At X=0.34 molar fraction, the number of sCT molecules equals that of GM1.

(Figs. 7b and 7c). Notably, Matsubara et al. obtained similar images in an AFM study concerning the formation of spherical aggregates of Aβ-protein driven by high-density of GM1 [36].

When X > 0.6 the monolayer structure should be totally different and dominated by the big and abundant sCT molecules embedded in the monolayer, and the model of Fig. 7 doesn't apply. However, we are not interested in this structure because very far from the biological conditions we are investigating.

4. Conclusions

To gain information about the effect of different lipid compositions on binding and aggregation of amyloid proteins to model membranes, we have prepared and studied a model mimicking some properties of the peculiar structures named lipid-rafts, or detergent resistant membranes, generally localized in the outer leaflet of the bilayer.

sCT was selected as the amyloid protein of choice for this study. Previously, we extensively studied this protein due to its noticeably slow aggregation rate, a characteristic that significantly facilitate sample preparation and stability, and allowed us to follow the protein-protein and protein-lipid interactions since the early stages [4,41,45,46].

We elaborated a combined biophysical approach; AFM, BAM microscopies measurements were applied to study the bilayer models, while the Langmuir trough technique to investigate the thermodynamic of the interaction of sCT with the outer membrane leaflet of the model. Finally, ζ-potential experiments were performed on liposomes to investigate the electrostatic nature of the interaction.

We found that the interaction between sCT and the model systems was controlled by the occurrence of GM1 and was of electrostatic nature. In particular, there is an indication of a preferential interaction between GM1 and sCT molecules, stabilized by Chol, with the result of the formation of a complex. The GM1 molecules represent the skeleton of the lipid-raft that drives the formation of spherical amyloid aggregates outside the bilayer.

Interestingly, similar models have been proposed for Aβ and other amyloid proteins, such as Aβ and prion. Thus, considering that a common structural arrangement has been hypothesized for different amyloid proteins, we support the idea that a common interaction mechanism for amyloid proteins interacting with lipid membranes rich in GM1 could exist. This outcome could hence provide useful information to design new therapeutic approaches of amyloid diseases based on the alteration of a membrane molecule like GM1 obtained, as an example, by cutting parts of the sialic acids by neuroaminidase and/or removing Chol by cyclodextrin.

Appendix A. Transparency document

Transparency data associated with this article can be found in the online version at http://dx.doi.org/10.1016/j.bbrep.2016.10.005.

References

[1] J. Schnabel, The dark side of proteins, Nature 464–8 (2010) 828–829.
[2] L. Goldschmidt, P.K. Teng, R. Riek, D. Eisenberg, Identifying the amylome, proteins capable of forming amyloid-like fibrils, Proc. Natl. Acad. Sci. USA 107–8 (2010) 3487–3492.
[3] H.A. Lashuel, P.T. Lansbury Jr., Are amyloid diseases caused by protein aggregates that mimic bacterial pore-forming toxins?, Q. Rev. Biophys. 39–2 (2006) 167–201.
[4] M. Diociaiuti, L. Zanetti-Polzi, L. Valvo, F. Malchiodi-Albedi, C. Bombelli, M.C. Gaudiano, Calcitonin forms oligomeric pore-like structures in lipid membranes, Biophys. J. 91 (2006) 2275–2281.
[5] R. Rakez-Kayed, A. Pensalfini, L. Margol, Y. Sokolov, F. Sarsoza, E. Head, J. Hall, C. Glabe, Annular protofibrils are a structurally and functionally distinct type of amyloid oligomer, J. Biol. Chem. 284- (7) (2009) 4230–4237.
[6] M. Bucciantini, E. Giannoni, F. Chiti, F. Baroni, L. Formigli, N. Zurdo, N. Taddei, G. Ramponi, C.M. Dobson, M. Stefani, Inherent toxicity of aggregates implies a common mechanism, Nature 416 (2002) 507–511.
[7] F. Chiti, C.M. Mobson, Protein misfolding, functional amyloid, and human disease, Biochemistry 75 (2006) 333–366.
[8] B.L. Kagan, R. Azimov, R. Azimova, Amyloid peptide channels, J. Membr. Biol. 202 (2004) 1–10.
[9] D. Schubert, C. Behl, R. Lesley, A. Brack, R. Dargusch, Y. Sagara, H. Kimura, Amyloid peptides are toxic via a common oxidative mechanism, Proc. Natl. Acad. Sci. USA 92 (1995) 1989–1993.
[10] S.S. Wang, T.A. Good, D.L. Rymer, The influence of phospholipid membranes on bovine calcitonin peptide's secondary structure and induced neurotoxic effects, Int. J. Biochem. Cell. Biol. 37 (2005) 1656–1669.
[11] M. Diociaiuti, G. Macchia, S. Paradisi, C. Frank, S. Camerini, P. Chistolini, M.C. Gaudiano, T.C. Petrucci, F. Malchiodi-Albedi, Native metastable prefibrillar oligomers are the most neurotoxic species among amyloid aggregates, Biochim. Biophys. Acta 1842 (9) (2014) 1622–1629.
[12] D.A. Brown, E. London, Origin and structure of ordered lipid domains in biological membranes, J. Membr. Biol. 164 (1998) 103–114.
[13] A. Rietvald, K. Simons, The differential miscibility of lipids as the basis for the formation of functional membrane rafts, Biochim. Biophys. Acta 1376 (1998) 467–469.
[14] D.A. Brown, E. London, Structure and function of sphingolipid- and cholesterol-rich rafts, J. Biol. Chem. 275 (2000) 17221–17224.
[15] K. Simons, D. Toomre, Lipid rafts and signal transduction, Nat. Rev. (Mol. Cell. Biol.) (1) (2000) 31–39.
[16] E. London, D.A. Brown, Insolubility of lipids in triton X-100: physical origin and relationship to sphingolipid/cholesterol domains (rafts), Biochim. Biophys. Acta 1508 (2000) 182–195.
[17] E. London, Insights into lipid rafts structure and formation from experiments in model membranes, Curr. Opin. Struct. Biol. 12 (2002) 480–486.
[18] F.M. Goñi, A. Alonso, L.A. Bagatolli, R.E. Brown, D. Marsh, M. Prieto, J.L. Thewalt, Phase diagrams of lipid mixtures relevant to the study of membrane rafts, Biochim. Biophys. Acta 1781 (2008) 665–684.
[19] L.J. Pike, Growth factor receptors, lipid rafts and caveolae: an evolving story, Biochim. Biophys. Acta 1746 (2005) 260–273.
[20] S.G. Kimberly, S. Wu, Lipid raft: a floating island of death or survival, Toxicol. Appl.

Pharm. 259 (2012) 311–319.

[21] G. Radeva, F.J. Sharom, Isolation and characterization of lipid rafts with different properties from RBL-2H3 (rat basophilic leukaemia) cells, Biochem. J. 380 (2004) 219–230.

[22] G. Thakur, C. Pao, M. Micic, S. Johnson, R.M. Leblanc, Surface chemistry of lipid raft and amyloid Aβ (1-40) Langmuir monolayer, Colloid Surf. B. 87 (2011) 369–377.

[23] K. Korade, A.K. Kenworthy, Lipid rafts, cholesterol and the brain, Neuropharmacology 55 (2008) 1265–1273.

[24] V. Michel, M. Bakovic, Lipid rafts in health and disease, Biol. Cell 99 (2007) 129–140.

[25] F. Malchiodi-Albedi, S. Paradisi, A. Matteucci, C. Frank, M. Diociaiuti, Amyloid oligomer neurotoxicity, calcium dysregulation, and lipid rafts, Int. J. Alzheimers Dis. 2011 (2011) 906964.

[26] B. Alberts, A. Johnson, J. Lewis, M. Raff, K. Roberts, P. Walter, Molecular Biology of the Cell, 4th edition, Garland Science, New York, 2002.

[27] K. Simons, E. Ikonen, Functional rafts in cell membranes, Nature 387 (1997) 569–572.

[28] D.A. Brown, J.K. Rose, Sorting of GPI-anchored proteins to glycolipid-enriched membrane subdomains during transport to the apical cell surface, Cell 68 (1992) 533–544.

[29] A. Pralle, P. Keller, E.L. Florin, K. Simons, J.K. Hörber, Sphingolipid- cholesterol rafts diffuse as small entities in the plasma membrane of mammalian cells, J. Cell. Biol. 148 (2000) 997–1007.

[30] J. Majewski, T.L. Kuhl, K. Kjaer, G.S. Smith, Packing of ganglioside-phospholipid monolayers: an x-ray diffraction and reflectivity study, Biophys. J. 81 (2001) 2707–2715.

[31] T. Ariga, K. Kobayashi, A. Hasegawa, M. Kiso, H. Ishida, T. Miyatake, Characterization of high-affinity binding between gangliosides and amyloid beta-protein, Arch. Biochem. Biophys. 388 (2001) 225–230.

[32] A. Kakio, S. Nishimoto, Y. Kozutsumi, K. Matsuzaki, Formation of a membrane-active form of amyloid-β protein in raft-like membrane, Biochem. Biophys. Res. Commun. 303 (2003) 514–518.

[33] A. Kakio, S. Nishimoto, K. Yanagisawa, Y. Kozutsumi, K. Matsuzaki, Cholesterol-dependent formation of GM1 ganglioside-bound amyloid-protein, an endogenous seed for Alzheimer amyloid, J. Biol. Chem. 276 (2001) 24985–24990.

[34] A. Kakio, S. Nishimoto, K. Yanagisawa, Y. Kozutsumi, K. Matsuzaki, Interactions of amyloid beta-protein with various gangliosides in raft-like membranes: importance of GM1 ganglioside-bound form as an endogenous seed for Alzheimer amyloid, Biochemistry 41 (2002) 7385–7390.

[35] K. Ikeda, T. Yamaguchi, S. Fukunaga, M. Hoshino, K. Matsuzaki, Mechanism of amyloid β-protein aggregation mediated by GM1 ganglioside clusters, Biochemistry 50 (29) (2011) 6433–6440.

[36] T. Matsubara, K. Iijima, N. Yamamoto, K. Yanagisawa, T. Sato, Density of GM1 in nanoclusters is a critical factor in the formation of a spherical assembly of amyloid β-protein on synaptic plasma membranes, Langmuir 29 (2013) 2258–2264.

[37] M. Manna, C. Mukhopadhyay, Binding, conformational transition and dimerization of amyloid-β peptide on GM1-containing ternary membrane: insights from molecular dynamics simulation, PLoS One 8 (8) (2013) e71308.

[38] J. Fantini, N. Yahi, N. Garmy, Cholesterol accelerates the binding of Alzheimer's β-amyloid peptide to ganglioside GM1 through a universal hydrogen-bond-dependent sterol tuning of glycolipid conformation, Front. Physiol. 4 (120) (2013) 1–10.

[39] L. Botto, D. Cunati, S. Coco, S. Sesana, A. Bulbarelli, E. Biasini, L. Colombo, A. Negro, R. Chiesa, M. Masserini, P. Palestini, Role of lipid rafts and GM1 in the segregation and processing of prion protein, PLoS One 9 (5) (2014) e98344.

[40] M. Bucciantini, D. Nosi, M. Forzan, E. Russo, M. Calamai, L. Pieri, L. Formigli, F. Quercioli, S. Soria, F. Pavone, J. Savistchenko, R. Melki, M. Stefani, Toxic effects of amyloid fibrils on cell membranes: the importance of ganglioside GM1, FASEB J. 26 (2) (2012) 818–831.

[41] F. Malchiodi-Albedi, V. Contrusciere, C. Raggi, K. Fecchi, G. Rainaldi, S. Paradisi, A. Matteucci, M.T. Santini, M. Sargiacomo, C. Frank, M.C. Gaudiano, M. Diociaiuti, Lipid raft disruption protects mature neurons against amyloid oligomer toxicity, Biochim. Biophys. Acta 1802 (2010) 406–415.

[42] D.M. Findlay, V.P. Michelangeli, R.C. Orlowski, T.J. Martin, Biological activities and receptor interactions of des-Leu16 salmon and des-Phe16 human calcitonin, Endocrinology 112 (4) (1983) 1288–1291.

[43] P.J. Gilchrist, J.P. Bradshaw, Amyloid formation by salmon calcitonin, Biochim. Biophys. Acta 1182 (1993) 111–114.

[44] S.S. Wang, T.A. Good, D.L. Rymer, The influence of phospholipid membranes on bovine calcitonin peptide's secondary structure and induced neurotoxic effects, Int. J. Biochem. Cell. Biol. 37 (2005) 1656–1669.

[45] M. Diociaiuti, M.C. Gaudiano, F. Malchiodi-Albedi, The slowly aggregating salmon calcitonin: a useful tool for the study of the amyloid oligomers structure and activity, Int. J. Mol. Sci. (12) (2011) 9277–9295.

[46] M.C. Gaudiano, M. Colone, C. Bombelli, P. Chistolini, L. Valvo, M. Diociaiuti, Early stages of salmon calcitonin aggregation: effect induced by ageing and oxidation process in water and in the presence of model membranes, Biochim. Biophys. Acta-Proteins Proteom. 1750 (2005) 134–145.

[47] M. Diociaiuti, F. Bordi, A. Motta, A. Carosi, A. Molinari, G. Arancia, C. Coluzza, Aggregation of gramicidin A in phospholipid Langmuir-Blodgett monolayers,

Biophys. J. 82 (2002) 3198–3206.

[48] H. Mohwald, Phospholipid and phospholipid-protein monolayers at the air/water interface, Annu. Rev. Phys. Chem. 41 (1990) 441–476.

[49] H.M. McConnell, Structures and transitions in lipid monolayers at the air-water interface, Annu. Rev. Phys. Chem. 42 (1991) 171–195.

[50] C.M. Knobler, R.C. Desai, Phase transitions in monolayers, Annu. Rev. Phys. Chem. 43 (1992) 207–236.

[51] A. Sorrenti, M. Diociaiuti, V. Corvaglia, P. Chistolini, G. Mancini, Chiral recognition of dipeptides in Langmuir monolayers, Tetrahedron.: Asymmetry 20 (23) (2009) 2737–2741.

[52] R. Maget-Dana, The monolayer technique: a potent tool for studying the interfacial properties of antimicrobial and membrane-lytic peptides and their interactions with lipid membranes, Biochim. Biophys. Acta 1462 (1999) 109–140.

[53] S. Pérez-López, M. Nieto-Suárez, C. Mestres, M.A. Alsina, I. Haro, N. Vila-Romeu, Behaviour of a peptide sequence from the GB virus C/hepatitis G virus E2 protein in Langmuir monolayers: its interaction with phospholipid membrane models, Biophys. Chem. 141 (2–3) (2009) 153–161.

[54] L. Caseli, R.G. Oliveira, D.C. Masui, R.P. Furriel, F.A. Leone, B. Maggio, M.E. Zaniquelli, Effect of molecular surface packing on the enzymatic activity modulation of an anchored protein on phospholipid Langmuir monolayers, Langmuir 21 (9) (2005) 4090–4095.

[55] T. Kamilya, P. Pal, G.B. Talapatra, Interaction of ovalbumin with phospholipids Langmuir-Blodgett film, J. Phys. Chem. B. 111 (5) (2007) 1199–1205.

[56] L. Dubreil, V. Vié, S. Beaufils, D. Marion, A. Renault, Aggregation of puroindoline in phospholipid monolayers spread at the air-liquid interface, Biophys. J. 85 (4) (2003) 2650–2660.

[57] M. Diociaiuti, I. Ruspantini, C. Giordani, F. Bordi, P. Chistolini, Distribution of GD$_3$ in DPPC monolayers: a thermodynamic and atomic force microscopy combined study, Biophys. J. 86 (2004) 321–328.

[58] G. Kamel, F. Bordi, L. Chronopoulou, S. Lupi, C. Palocci, S. Sennato, P.V. Verdes, Adsorption of Candida rugosa lipase at water-polymer interface: the case of poly(dl) lactide, Surf. Sci. 605 (2012) 2017–2024.

[59] G. Thakur, M. Micic, R.M. Leblanc, Surface chemistry of Alzheimer's disease: a Langmuir monolayer approach, Colloid Surf. B. 74 (2) (2009) 436–456.

[60] E.E. Ambroggio, D.H. Kim, F. Separovic, C.J. Barrow, K.J. Barnham, L.A. Bagatolli, G.D. Fidelio, Surface behavior and lipid interaction of Alzheimer beta-amyloid peptide 1-42: a membrane-disrupting peptide, Biophys. J. 88 (4) (2005) 2706–2713.

[61] E. Prenner, G. Honsek, D. Hönig, D. Möbius, K. Lohner, Imaging of the domain organization in sphingomyelin and phosphatidylcholine monolayers, Chem. Phys. Lipids 145 (2) (2007) 106–118.

[62] T. Gröger, S. Nathoo, T. Ku, C. Sikora, R.J. Turner, E.J. Prenner, Real-time imaging of lipid domains and distinct coexisting membrane protein clusters, Chem. Phys. Lipids 165 (2) (2012) 216–224.

[63] M. Diociaiuti, F. Bordi, A. Motta, A. Carosi, A. Molinari, G. Arancia, C. Coluzza, Aggregation of gramicidin A in phospholipid Langmuir-Blodgett monolayers, Biophys. J. 82 (2) (2002) 3198–3206.

[64] N.R. Pallas, B.A. Pethica, Liquid-expanded to liquid-condensed transition in lipid monolayers at the air/water interface, Langmuir 1 (4) (1985) 509–513.

[65] A. Blume, A comparative study of the phase transitions of phospholipid bilayers and monolayers, Biochim. Biophys. Acta - Biomemb. 557 (1) (1979) 32–44.

[66] D.K. Chattoraj, K.S. Birdi, Adsorption and the Gibbs Surface Excess, Plenum Press, New York, 1984.

[67] M.J.G. Ruiz, M.A.C. Vílchez, A study of the miscibility of bile components in mixed monolayers at the air-liquid interface. I. Cholesterol, lecithin and lithocholic acid, Colloid Polym. Sci. 269 (1991) 77–84.

[68] M. Hope, R. Nayar, L.D. Mayer, P. Cullis, Reduction of liposomes size and preparation of unilamellar vesicles by extrusion techniques, in: G. Gregoriadis (Ed.) 2nd ed., Liposome Technology vol. 1, CRC Press, Boca Raton, FL, 1992, pp. 123–139.

[69] R. MacDonald, R. MacDonald, Applications of freezing and thawing in liposomes technology, in: G. Gregoriadis (Ed.)2nd ed., Liposome Technology vol. 1, CRC Press, Boca Raton, FL, 1992, pp. 209–228.

[70] C.L. Lawson, I.D. Morrison, Solving Least Squares Problems. A FORTRAN Program and Subroutine Called NNLS, Prentice-Hall, Englewood Cliffs, NJ, 1974.

[71] C. De Vos, L. Deriemaeker, R. Finsy, Quantitative assessment of the conditioning of the inversion of quasi-elastic and static light scattering data for particle size distributions, Langmuir 12 (1996) 2630–2636.

[72] W.W. Tscharnuter, Mobility measurements by phase analysis, Appl. Opt. 40 (24) (2001) 3995–4003.

[73] N.V. Romeu, P. Dynarowicz-Łatka, J.M. Trillo, J.R. Seoane, O. Conde-Mouzo, Kinetics of destabilization of calcitonin monolayers at the air/water interface, J. Colloid Interface Sci. 198 (1) (1998) 179–182.

[74] N.V. Romeu, J.M. Trillo, O. Conde, M. Casas, E. Iribarnegaray, Influence of several factors on the response of calcitonin monolayers to compression at the air-water interface, Langmuir 13 (1997) 71–75.

[75] M.N. de Mul, J.A. Mann, Determination of the thickness and optical properties of a langmuir film from the domain morphology by brewster angle microscopy, Langmuir 14 (1998) 2455–2466.